

BIOMETRIC IDENTIFICATION WITH 3D FINGERPRINTS ACQUIRED THROUGH OPTICAL COHERENCE TOMOGRAPHY

Henrique Sérgio Gutierrez da Costa*, Olga R.P. Bellon[†] and Luciano Silva[‡],
IMAGO Research Group, Universidade Federal do Paraná - Curitiba, Brazil
e-mail: hsgcosta@inf.ufpr.br, olga@ufpr.br, luciano@ufpr.br

Abstract—A method to obtain epidermal and dermal 3D fingerprints from high-resolution images acquired using Optical Coherence Tomography (OCT) is proposed. This method addresses limitations of current 3D reconstruction techniques such as depth and resolution variations, sensitivity to low illumination and poor contrast. The availability of these fingerprints made possible the creation of new identification techniques that benefit from the rich information available in 3D. We propose a 3D fingerprint matching process based on KH maps, which are 2D representations of curvature types extracted by computing the Gaussian and mean curvatures from a region of interest around minutiae. The matching strategy, a two-step approach, relies on local gradient patterns (LGP) of the KH maps to narrow the search space, followed by a similarity matching, normalized cross correlation. The accuracy and matching compatibility, comparable or improved in relation to the 2D matching methods, is verified through matching 3D fingerprints from two databases one acquired using OCT and a public database. An OCT 3D fingerprint database, the first acquired this technology to our knowledge, contains images of people of different ages, genders, ethnicity and cases of alterations as scars, abrasion and scratches. We investigate the applicability of our method to the identification of altered fingerprints. In these cases, the 3D dermal fingerprint, compatible with the epidermis, is employed.¹

Keywords—3D fingerprints; biometric identification; OCT

I. INTRODUCTION

Person identification has been used for many years in commercial, governmental and legal applications and has been adopted in large scale worldwide. A particular application, gaining importance due to the increasing number of identification deception attempts [1], is border control and access to security facilities.

2D fingerprint technologies have been successfully used for years but despite the continuous progress, opportunities for improvement remain. An important issue is vulnerability to skin alterations, unintentional as in the cases of abrasion and scratches related to some types work, or deliberate, as the cases of acid burns and plastic surgery with the purpose of evading the identification by a biometric system, as described by Yoon and Jain [1]. Another case of relevance is the identification of newborn babies, a challenging problem due to its high deformability, the small dimensions of their dermatoglyphics (2 to 3 times smaller than in adults). Skin deformability was attributed to the small thickness of the epidermis and

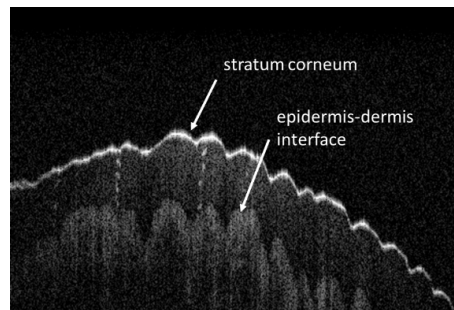


Fig. 1. B-Scan of the finger skin showing the stratum corneum and the dermis-epidermis interface

can be prevented by contactless scanning. Lastly, it has been estimated that 4% of the population may have poor skin ridge quality making it very difficult or impossible to scan these fingerprints.

3D fingerprint geometry has been studied as a promising alternative to 2D identification technologies as it provides richer, discriminatory information obtained through contactless imaging and 3D reconstruction. However, despite its inherent advantages as the immunity to skin deformation, it has been limited to superficial images of the skin, impacted by illumination, brightness, contrast, and errors inherent to triangulation or phase-calculation. The use of 3D scanners that provide the spatial information directly, with no reconstruction need can potentially minimize the errors inherent to these techniques. By working with the 3D information, one can extract some discriminant characteristics such as curvatures.

A new method to obtain 3D fingerprints from images of the dermis and epidermis, acquired through OCT is proposed. OCT, a contactless high-resolution scanning technology that acquires in-depth 3D images of the skin layers provides access to the internal structures of the skin (Fig.1), exposing structures that can be potentially be used to improve identification/verification. The resolutions obtained (of microns) are sufficient to scan newborn babies fingerprints and the information available in the dermis-epidermis interface can make biometric identifications viable when the epidermis has been altered. In addition, the skin intensity profile and the internal structures of the skin can be used to detect fake fingerprints. In the proposed method, 3D fingerprints are extracted

¹PhD Thesis

from the epidermis and dermis-epidermis OCT images in a region of interest (ROI), a small point cloud around fingerprint minutiae, named minutiae cloud. From this ROI, the KH maps, distinctive information used for biometric identification is calculated. The use of multiple minutiae clouds can improve the accuracy of the biometric identification if compared to the traditional 2D methods. A database of epidermal and dermal OCT 3D fingerprints, the first to our knowledge, was built by scanning images of 11 volunteers in 2 sessions held in different days through a partnership with Stanford University, where an OCT scanner was made available.

A method for fingerprint matching based on the mentioned novel patterns is also presented. The KH maps used for matching are computed from minutiae clouds based on signs of the Gaussian and mean curvatures as proposed by Besl and Jain [2]. Large databases of KH maps, one for each minutiae cloud, can be built, what can impact the matching response time. The matching strategy, a two-step approach relies on local gradient patterns (LGP) of the KH maps to mitigate this problem by narrowing the search space, followed by a similarity matching of the nearest neighbors of the pattern being searched. The accuracy and matching compatibility, comparable or improved in relation to the 2D matching methods is verified through matching using epidermis-epidermis and epidermis-dermis minutiae clouds and comparing the results (FARx_{FRR}, ROC and CMC curves) with those obtained for traditional 2D fingerprint matching collected from the same volunteers.

II. BIOMETRIC IDENTIFICATION USING FINGERPRINTS

Fingerprint identification is based on dermatoglyphics, finger skin patterns present in the skin, such as the ridges, valleys and minutiae are used. Fingerprints are formed by the detection of these dermatoglyphics by an image sensor or ink and paper. The skin consists of the epidermis and dermis layers. The epidermis is a layered structure, being the stratum corneum, the outermost. Deeper in the skin, the epidermal-dermal interface has irregularities that are named dermal papillae. These mold the formation of the epidermal ridges during the fetus formation [3], making these two regions very similar in shape.

2D fingerprint technologies have been successfully used for decades, being considered mature and reliable but they have limitations. One of them is the impact of skin deformation and the presence of dirt and moisture during the image acquisition, which can impact the identification accuracy. Another, is the vulnerability to biometric system obfuscation by finger skin alterations. These can occur for unintentional reasons as the constant use of the hands in labor activities [4] or intentional, to try to mask a person identity through burns, cuts, abrasion and even plastic surgery. These changes can modify the shape of the fingerprints scanned by traditional, contact-based or even contactless scanners and deceive the automatic identification systems [1]. Recently, research on the use 3D fingerprints from images acquired with multiple cameras or structured light systems have been proposed but

depth and resolution problems occurred. Improved matching results have only been obtained when the scores are combined with those obtained through 2D fingerprint matching.

III. ACQUISITION OF 3D FINGERPRINTS

3D acquisition systems have been proposed in the literature: in [5] a touchless scanner with 5 cameras and 16 LEDs obtains 3D reconstructed images using stereovision and photogrammetry-based algorithms. Matching employs 2D and 3D features: 2D unwrapped images (from the 3D fingerprints) are matched against existing 2D databases and the locations of correspondent spatial minutiae triplets are adopted for 3D matching. In [6], a sinusoidal pattern is projected by a digital light processing (DLP) device on the finger. The skin shape changes the phase of the projected pattern and the resulting image can be used for the computation of the spatial coordinates of each point. Errors of 0.0301 mm in depth and 0.0006 mm in x and 0.014mm in y were found.

Wang et al [7] uses structured light illumination and phase measuring profilometry to obtain a 3D reconstruction of the finger. An unwrapped 2D fingerprint is built through a parametric technique. In the work by Labati et al [8], whose focus was in the acquisition with moving fingers, two images are collected and enhanced to increase fringe contrast and correspondent points of the two images are found using block matching and normalized cross-correlation. A 3D shape is computed by triangulation using the coordinates of the corresponding points to build an image of the ridge pattern texture, that is superimposed to the 3D model. Unwrapped fingerprints are used for matching, having obtained ERR of 0.09% and FMR of 0.12%, that dropped to 2.40% and 1.2% when intentional misplacements and rotations are present. Compatibility of these with flat 2D fingerprints acquired through a regular 2D scanner was tested, the obtained ERR was 1.48% in the worst case. In this case, the 3D reconstructed model does not have the ridges and valleys depth information.

A different approach, using a single camera and 7 LEDs was described in [9] and [10]. 2D images obtained by synchronized flashing of the LEDs at different angles are used to build a 3D fingerprint using shape estimation with shape from shading, least squares and Poisson solver techniques. For matching, a shape index (SI) is adopted. This index is obtained by calculating the surface maximum and minimum curvatures and depending on its value, the surface can be segmented in five types (cup, rut, saddle, ridge, cap). SI is combined with the direction of the dominant principle curvature to form a vector named Finger Code (FC). Normalized Hamming distance between FCs is employed for 3D matching. Another matching approach used in the same paper relies on 3D coordinates of minutiae, including the height and angles in relation to a central minutia, combined with traditional 2D minutiae-based matching. A database of 3D fingerprints from 240 users containing 3D and 2D fingerprints was built using the proposed acquisition method. 3D fingerprint matching through curvatures (SI) obtained an ERR of 15.56% but best matching results were reached when 3D minutiae scores were fused with

2D minutiae-based scores (adaptive fusion), achieving an ERR 1.02% [10].

In [11], the image is obtained through 3 cameras and 3 LEDs. 3D image reconstruction starts by estimating the finger shape, then SIFT features and minutiae correspondence between the collected 2D images are found and used to calculate the spatial coordinates of each point of the finger. These coordinates are superposed to the shape model to form the 3D fingerprint. Reconstruction errors of up to 0.35 mm were found. Curve skeletons extracted from these 3D images [12] are used for matching along with curvature maximum and minimum measures. Curvature shape matching alone resulted in EER of 15%, improved to 3.4% when the curvature measures were included.

A set of common problems found in the listed 3D reconstruction methods can be summarized as follows: depth, resolution and ridge variations from the center to the image borders; low overlapping regions among images from multiple cameras; poor illumination and low-contrast, affecting coordinate calculation.

IV. 3D FINGERPRINT ACQUISITION WITH OCT

OCT technology can generate 2D cross-sectional images (B-scans) and 3D images of the skin. It has been used in the biomedical area to image structures with submicron resolution [13]. In human skin, OCT images at depths of a few millimeters, have been reached [14], [15] and in biometric identification using the finger skin, detection of fake fingerprints has been reported [16], [17]. As OCT uses low time-coherent interferometry, no reconstruction is needed, the image of the skin layers is acquired directly from the sample with no resolution and depth variation from center to borders of the finger and illumination being contrast problems also prevented.

An example of cross-sectional OCT images of the skin is presented in Fig. 2.a (top), where the external part of the epidermis (stratum corneum) appears as a thin bright layer due to large refractive index mismatch between the air and the skin, as a consequence the ridges and valleys are clearly visible in these images. Deeper in the skin, the interface between epidermis-dermis has a structure whose shape is very similar to the stratum corneum [18] and visible as a lower intensity (if compared to the stratum corneum) section of the skin in the B-scans as the refractive index mismatch is not so large. By detecting the interfaces between the stratum corneum/air and the dermis/epidermis, two point clouds, the 3D dermal and epidermal fingerprints can be built.

A. 3D Fingerprint extraction

OCT finger images are processed to generate the 3D epidermis fingerprint (external) from the stratum corneum and the 3D dermal fingerprint (internal) from the epidermis-dermis interface. Different methods are adopted for external and internal 3D fingerprints. For the external, since the stratum corneum is a high-intensity sharp line, Canny edge detector

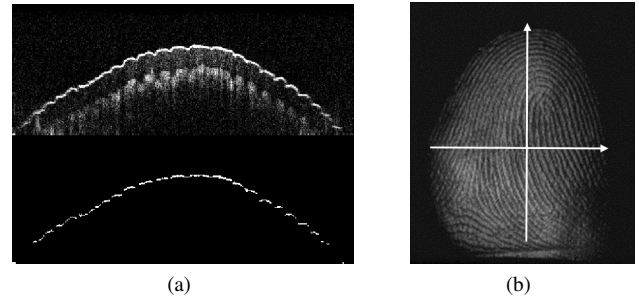


Fig. 2. Detection of external fingerprint: (a) Original (top) and detected external layer (bottom); (b) detection directions (white arrows).

is used as shown in Fig.2. Edge detection is executed in two orthogonal directions to increase the amount of points.

For internal 3D fingerprint, the intensity of dermis-epidermis interface is first enhanced by the method proposed by [19] that takes into consideration the intensity contribution of groups of neighbor points in this region. First a weighted median filter is applied to the B-scan, then for each column of the B-scan (represented by a white arrow in Fig.3) an intensity profile is built and the second intensity peak (second maximum in Fig.3 graph) is located. This corresponds to the epidermis-dermis interface. An edge detector is then applied to this image to obtain the 3D internal fingerprint.

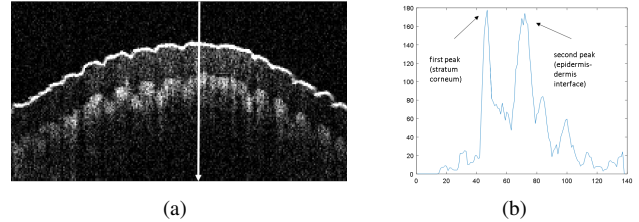


Fig. 3. Epidermis-dermis detection: (a) A-scan represented by the white arrow; (b) the intensity graph of the A-scan.

3D fingerprints are formed by stacking of all the detected edges, as shown in Fig.4.

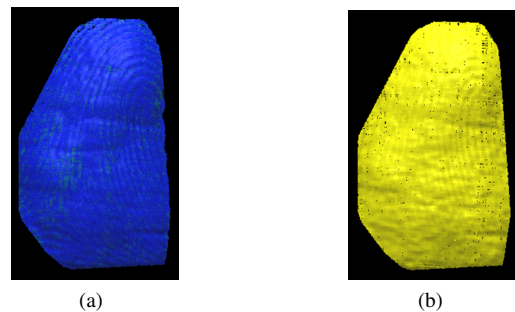


Fig. 4. 3D Fingerprints from OCT images: (a) External 3D fingerprint; (b) Internal 3D fingerprint

B. OCT 3D Fingerprint database (OCTDB)

A 3D fingerprint database was acquired through a partnership with Stanford University and followed an approved acquisition protocol. 3D images were scanned using a general-purpose OCT with a field of view of 14.1 mm X 14.1 mm and a resolution of 7.5m (equivalent to approximately 1170 ppi). Volumes of 700 x 700 x 256 voxels were obtained from 11 volunteers in two scanning sessions and occurred in different days. The 10 fingers of each volunteer were scanned and when needed, additional scans were done if motion artifacts (by involuntary motion) were observed. A total of 163 3D internal and external fingerprints were obtained. The processed images formed the first OCT 3D fingerprint database (referred as OCTDB) to our knowledge. In addition, 2D images of the fingerprints using a regular contact-based scanner were scanned from the same volunteers. This database differs from the others acquired by the other technologies by the higher resolution, clearly defined ridges and valleys, accurate scanning of all the skin irregularities and the availability of the internal structures as the epidermis, dermis, sweat ducts and dermal papillae. Its use in future research can open the exploitation of new biometric features and innovative matching methods as the one proposed in the next session.

C. ROI Extraction to Matching

Our proposed matching process uses regions of the 3D cloud around the minutiae, considered distinctive regions of the finger. These were extracted selecting a frame of 150x150 pixels (X-Y) centered in the minutiae coordinates to obtain the region of interest (ROI), named *minutia cloud* (Fig. 5.a). Only the minutiae types bifurcations and endings were used in this experiment.

Minutiae clouds acquired in the first scanning session were stored in the gallery group and those acquired in the second session in the probe group. Probe represents the enrolled minutiae clouds of a user to be identified by searching the minutiae clouds stored in the gallery. Minutiae clouds are convenient to matching as their configuration makes them very distinctive from mere ridges and are found in reasonable amounts in the fingers. They are used to calculate our distinctive features, the KH maps (Fig 5.b), obtained from the Gaussian and Mean curvatures of point clouds.

D. KH Maps

KH maps (Fig.5) are obtained from the minutiae cloud by the following steps: (1) Gaussian smoothing; (2) interpolation of the 3D points in a regular grid; (3) computing curvature values for each 3D point; and (4) converting the curvature values to the 2D KH map. The regular grid is based on the useful area of the 3D minutia cloud. Finally, the regions are segmented by curvature type and different greyscale intensities (10, 30, 70 and 90) are attributed to the curvature types of each minutiae cloud segment for visualization, showing that different segments have clear separation edges.

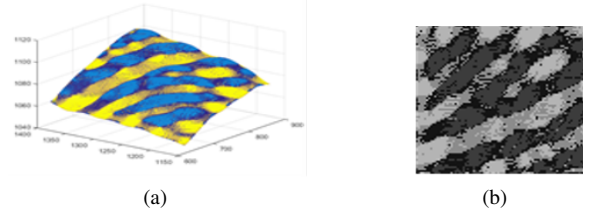


Fig. 5. Minutiae clouds and correspondent KH Map: (a) Minutiae cloud rendered image ; (b) KH Map

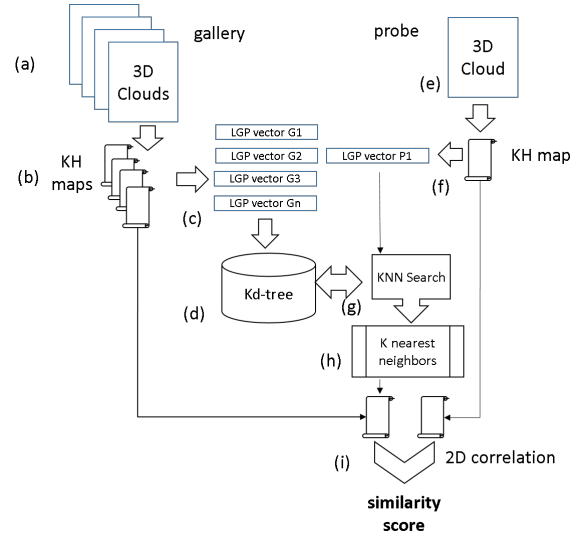


Fig. 6. 3D Fingerprint Matching process

V. 3D FINGERPRINT MATCHING

Our two-step 3D fingerprint matching method [20] starts by extracting the minutiae clouds, from the full 3D fingerprint image. Follows the computation of the KH maps, their local gradient patterns and the final score calculation (2D correlation). Two sets of KH maps are used: 1) the gallery, resulting from the 3D fingerprints scanned in the first session, simulating the enrollment stage and the 2) probe, composed of the 3D fingerprints scanned in the second session, representing the case of a user having its 3D fingerprints scanned to identification. Samples of the probe KH-maps are matched against the gallery. Fig. 6 shows an overview of the matching process. After the KH maps are calculated, a texture descriptor for each of them is computed, Local Gradient Patterns (LGP) [21] followed by a similarity calculation through normalized cross-correlation of the KH-maps.

LGPs are obtained for each point of the KH maps first calculating the intensity gradient g_i of it to its p closest neighbors (in absolute value), then obtaining the average of these gradients and attributing a value S_i (0 or 1) corresponding to each neighbor. S_i values are concatenated to form the LGP value for each pixel, a p -bits number. The image is then divided in 25 sections and the histogram of LGP values for each section is computed and concatenated to form a representative vector. This vector is generated for each gallery

KH map. The whole set of vectors is stored as a Kd-Trees (gallery database) that will be used to matching. Kd-Trees contribute to reduce the search space when trying to search correspondences in gallery database, making the identification faster.

The probe minutiae cloud, extracted from the 3D fingerprints of the person to be identified, has its KH map calculated, its finger type determined and LGP descriptor built. Then a KNN search on the Kd-Tree returns the K closest neighbors using Euclidean distance. Finally, the 2D correlation is executed between the probe KH map and all the K closest neighbors to determine the similarity score (normalized cross-correlation) used for matching. The matching process is repeated for all the minutiae clouds found in each finger (probe) and a score S for all the Rank-1 matches is calculated. The FARx \bar{F} RR, CMC and ROC curves are plotted based on the S score to evaluate the accuracy of the method for single and multiple minutiae.

VI. EXPERIMENTS AND MATCHING RESULTS

We measured the matching accuracy using two databases, the OCTDB and a public database. In addition, we evaluated the compatibility of the minutiae clouds extracted from the dermis-epidermis interface and epidermis to check if dermis 3D fingerprint can be used when the epidermis is altered or it is inaccessible.

A. 3D Fingerprint Database from Hong Kong Polytechnic

A public database gently made available by the Hong Kong Polytechnic University, [9], referred as POLYUDB in this work, was used in tests to check the method applicability and to compare with OCTDB results. This database has around 1,560 3D images from 260 subjects. In our work we selected 88 images from 44 subjects, the ones that had clear definition of curvature types as opposed to images excessively smoothed and showing artifacts.

B. KH Map Matching (CORR2D)

A test with KH maps from different fingers (and users) was executed to evaluate the accuracy of the method by first trying to match a single minutia cloud from the probe to the ones in the gallery to evaluate how accurate the use of a single minutiae cloud was for identifying a finger. After that, matching was applied using whole set of minutiae clouds found for each the finger in order to measure the improvement in matching accuracy.

C. Tests with the OCTDB Database

Tests using 3,945 minutiae from OCTDB were executed to evaluate the matching accuracy. 86 fingers from the probe were matched. On average 4.12 minutiae clouds per finger were found. The resulting FARx \bar{F} RR and CMC curves, are shown in Fig.7 (left). First test (single minutia) resulted in an EER (equal error rate) of 12.77% and an identification rate of 75% for Rank-1. In the second test (multiple minutiae clouds) an ERR of 3.8% was obtained and an identification

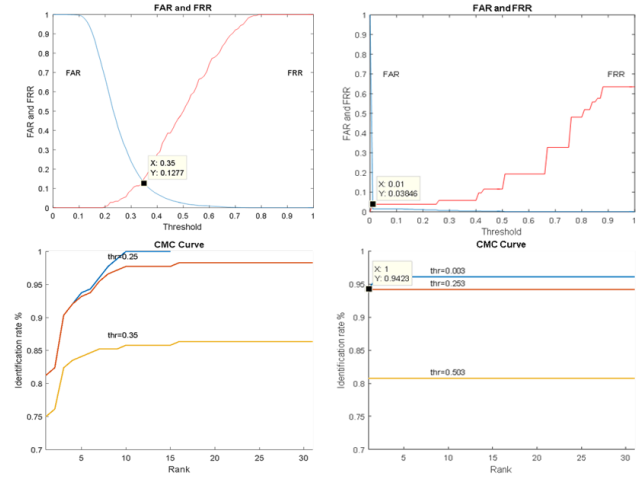


Fig. 7. FAXx \bar{F} RR and CMC curves (OCTDB): (left) single minutia; (right) multiple minutiae

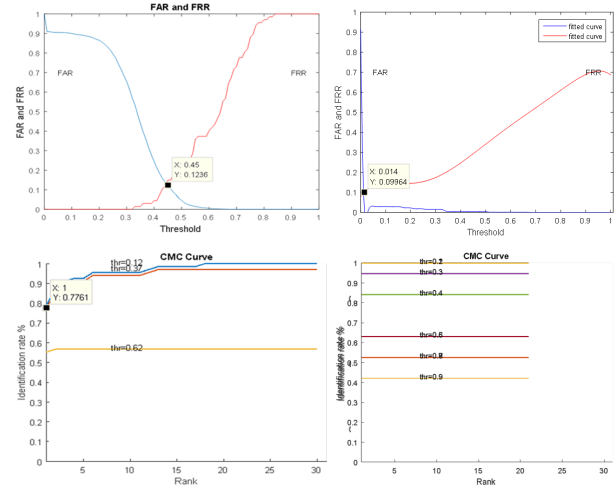


Fig. 8. FAXx \bar{F} RR and CMC curves (POLYUDB): (left) single minutia; (right) multiple minutiae

rate of 94.23% as shown in Fig.7 (right), showing a significant improvement on both the EER and the identification rates.

D. Tests with POLYUDB database

Tests using 350 minutiae clouds extracted from 86 3D fingerprints of 43 volunteers from POLYUDB were executed. An average of 3.97 minutiae clouds per finger was found. As in the previous database tests, single and multiple minutia cloud tests were run. For single minutiae, an EER of 12.36% and a CMC curve with 77.61% recognition rate was found as in Fig.8 (left). For multiple minutiae, a significant improvement was found an ERR of 9.96% and an identification rate 99% for Rank-1 as in Fig.8 (right). A comparison of the EER and identification rates obtained for the OCTDB and POLYUDB show that EER and identification rates are similar for a single minutia but for multiple minutiae, EER is better for OCTDB than for POLYUDB and the identification rate is better for POLYUDB than for OCTDB.

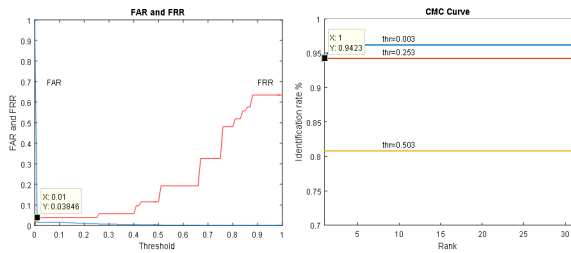


Fig. 9. FAXxERR and CMC curves (OCTDB) for External x Internal

E. Compatibility of 3D Dermal and Epidermal Fingerprints

The hypothesis that the internal (dermal) 3D fingerprints can be used for matching when the epidermal fingerprint is not available [18] is tested. Images from 3D epidermis x dermis fingerprints from the gallery and probe sets were selected. A total of 11 fingers from 5 volunteers and a total of 52 minutiae clouds were used. As can be seen in Fig. 9, the resulting FAXxERR and CMC curves show an EER of 0.6% and an identification rate of 88.89% (Rank-1). The identification rate obtained using the dermis is typically inferior to regular 2D due to the smaller percentage of minutiae coincidence between the epidermis and dermis. However, the identification rate obtained was superior to the results obtained by traditional invasive process used in identification of corpses, (exposure of the dermis by chemical process) [18].

VII. CONCLUSIONS

The acquisition of 3D fingerprints obtained through the use of OCT was proved viable and the first OCT 3D fingerprint database to date was built, containing 163 internal and external 3D fingerprints. This database allows the exploitation of features as the curvatures and new structures as papillary glands and sweat ducts for improved matching. OCT has a series of advantages over the triangulation-based and structured illumination profilometry-based systems such as the immunity to contrast, illumination problems and reconstruction errors. Besides that, the access to the internal layers of the skin opens the possibility to do biometric identification in the presence of alterations or when the external layer of the skin is not accessible. A new matching method based on KH maps, computed from the minutiae clouds, was proposed to improve the identification accuracy. A two-step LGP-based matching process was devised to cope with the large volume of minutiae clouds and reduce the processing time. The matching results, for OCTDB and POLYUDB were obtained and a comparison with 2D traditional matching was executed. Identification rates of 75% and 77.61% and ERR of 12.77% and 12.36% for respectively the OCTDB and POLYUDB for a single minutiae cloud and 94.23% and 99% for an ERR of 3.9% and 9.96% for multiple minutiae were achieved. The case of matching an external 3D database using internal fingerprints has been tested obtaining identification rate of 88.89% and EER of 0.06% showing that identification is feasible in the case of alterations or when the external layer cannot be acquired.

REFERENCES

- [1] S. Yoon, J. Feng, and A. K. Jain, "Altered fingerprints: analysis and detection," *IEEE Transactions on Pattern Analysis and Machine Intelligence*, vol. 34, no. 3, pp. 451–64, mar 2012.
- [2] P. J. Besl and R. Jain, "Invariant Surface Characteristics for 3D Object Recognition in Range Images," *Computer Vision, Graphics and Image Processing*, vol. 33, pp. 33–80, 1986.
- [3] H. Cummins and C. Midlo, *Finger Prints, Palms and Soles*. Dover Publications Inc., 1976.
- [4] J. Feng, A. K. Jain, and A. Ross, "Detecting Altered Fingerprints," *2010 20th International Conference on Pattern Recognition*, pp. 1622–1625, aug 2010.
- [5] G. Parziale, E. Diaz-santana, and R. Hauke, "The Surround Imager : a multi-camera touchless device to acquire 3D rolled-equivalent fingerprints," *International Conference on Advances in Biometrics, ICB 2006*, vol. LNCS 3832, pp. 244–250, 2005.
- [6] S. Huang, Z. Zhang, Y. Zhao, J. Dai, C. Chen, Y. Xu, E. Zhang, and L. Xie, "3D fingerprint imaging system based on full-field fringe projection profilometry," *Optics and Lasers in Engineering*, vol. 52, pp. 123–130, 2014.
- [7] Y. Wang, L. G. Hassebrook, and D. L. Lau, "Data acquisition and processing of 3-D fingerprints," *IEEE Transactions on Information Forensics and Security*, vol. 5, no. 4, pp. 750–760, 2010.
- [8] R. D. Labati, A. Genovese, V. Piuri, and F. Scotti, "Toward Unconstrained Fingerprint Recognition : A Fully Touchless 3-D System Based on Two Views on the Move," *IEEE Transactions on Systems, Man and Cybernetics*, vol. 46, no. 2, pp. 202–219, 2016.
- [9] A. Kumar and C. Kwong, "Towards contactless, low-cost and accurate 3D fingerprint identification," in *Proceedings of the IEEE Computer Society Conference on Computer Vision and Pattern Recognition*, vol. 37, no. 3, 2013, pp. 3438–3443.
- [10] —, "Towards Contactless , Low-Cost and Accurate 3D Fingerprint Identification," *IEEE Transactions on Pattern Analysis and Machine Intelligence*, vol. 37, no. 3, pp. 681–696, jun 2015.
- [11] F. Liu and D. Zhang, "3D fingerprint reconstruction system using feature correspondences and prior estimated finger model," *Pattern Recognition*, vol. 47, no. 1, pp. 178–193, 2014.
- [12] F. Liu, D. Zhang, and L. Shen, "Study on novel Curvature Features for 3D fingerprint recognition," *Neurocomputing*, pp. 1–10, 2015.
- [13] G. Bouma, B.E.Tearney, *Handbook of Optical Coherence Tomography*. New York: Marcel Dekker AG, 2002.
- [14] P. Zakharov, M. S. Talary, I. Kolm, and A. Caduff, "Rapid skin profiling with non-contact full-field optical coherence tomography: Study of patients with diabetes mellitus type I," in *Proceedings of SPIE-OSA Biomedical Optics - Optical Coherence Tomography and Coherence Techniques*, vol. 7372. SPIE, 2009, p. Optical Society of America.
- [15] B.-W. Yang and X.-C. Chen, "Full-color skin imaging using RGB LED and floating lens in optical coherence tomography," *Biomedical optics express*, vol. 1, no. 5, pp. 1341–1346, jan 2010.
- [16] J. Galbally, R. Cappelli, A. Lumini, G. Gonzalez-de Rivera, D. Maltoni, J. Fierrez, J. Ortega-Garcia, and D. Maio, "An evaluation of direct attacks using fake fingers generated from ISO templates," *Pattern Recognition Letters*, vol. 31, no. 8, pp. 725–732, jun 2010.
- [17] Y. Cheng and K. V. Larin, "Artificial fingerprint recognition by using optical coherence tomography with autocorrelation analysis," *Applied optics*, vol. 45, no. 36, pp. 9238–45, dec 2006.
- [18] L. L. Mizokami, L. R. V. Silva, and S. A. S. Kückelhaus, "Comparison between fingerprints of the epidermis and dermis: Perspectives in the identifying of corpses," *Forensic Science International*, vol. 252, pp. 77–81, 2015.
- [19] M. R. Avnani and A. Hojjatoleslami, "Skin layer detection of optical coherence tomography images," *Optik - International Journal for Light and Electron Optics*, vol. 124, no. 22, pp. 5665–5668, nov 2013.
- [20] H. Costa, O. R. P. Bellon, L. Silva, and A. K. Bowden, "Towards Biometric Identification Using 3D Epidermal and Dermal Fingerprints," in *Proceedings of IEEE International Conference on Image Processing*, I. S. P. Society, Ed., Phoenix, 2016.
- [21] Z. Lubing and W. Han, "Local Gradient Increasing Pattern for Facial Expression Recognition," in *2012 19th IEEE International Conference on Image Processing*, Orlando, 2012, pp. 2601–2604.